Talanta 223 (2021) 121766

Contents lists available at ScienceDirect

Talanta

journal homepage: www.elsevier.com/locate/talanta

Plasma treated graphene FET sensor for the DNA hybridization detection

Yaping Xia [a], Yang Sun [a,b], Huamin Li [b], Shuo Chen [a], Tiying Zhu [a], Guangcan Wang [a], Baoyuan Man [a], Jie Pan [a,**], Cheng Yang [a,b,*]

[a] School of Physics and Electronics, Shandong Normal University, Jinan, 250014, People's Republic of China
[b] Department of Electrical Engineering, University at Buffalo North Campus, Buffalo, NY, 14260, USA

ARTICLE INFO

Keywords:
CVD graphene
Field-effect transistors
Plasma treatment
DNA hybridization detection
Charge neutral point

ABSTRACT

Room-temperature plasma treated graphene based FET was firstly proposed for the DNA hybridization detection. Affinity and electrical properties of the graphene based DNA-FET sensor were studied and improved benefits from the surface modification. The facile room-temperature Ar plasma easily removes residues from the graphene surface and changes the hydrophilic properties of graphene, which is important for our solution gated DNA-FET sensor. Limit of the detection of below 10 aM is obtained in our experiment. Especially, DNA concentration (C_{DNA})/the amount of net drain current (ΔI) and the negative shift in the V_{CNP} value of the GFET sensor with the plasma treated 30 s are all improved compared with that without treatment. It shows that the easily plasma treatment of the graphene surface can be used for the solution gated FET sensor.

1. Introduction

Plasma treatment of the novel two dimensional channel materials has been considered as a potential technology to improve the electrical properties of the FET devices [1–6]. Generally, the electronic properties of the two dimensional materials can be changed by the different plasma atmosphere. Plasma treatment under Ar inductively coupled plasma is proposed as an efficient method for cleaning the surface of two-dimensional materials to restore the performance degradation caused by PMMA passivation [4]. And $CF4/H_2$ plasma cleaning the residues (PMMA et al.) of graphene surface almost recovers the original properties of quasi-freestanding graphene [6]. In these, the Ar plasma could remove residues from materials surface without any risk of contamination and avoid high temperature. As well as, Ar gas would not be doped with the materials and not destroy the structure of materials [7,8]. In addition, the graphene samples treated by Ar plasma are more conductive than those treated by other plasma [9]. Therefore, plasma treatment under Ar gas is rather good way for surface modification of materials.

DNA, used as the carrier of biological genetic information, plays an extremely important role in organisms [10]. Through DNA hybridization detection, valuable medical diagnostic information can be obtained, which is beneficial to the early prevention and treatment of diseases [11–13]. Many methods including optical and electrochemical [14–18], surface plasmon resonance [19,20], and FET [21–27] have been reported for detecting DNA hybridization. Among them, solution gated FET sensors have been considered as one of the most potential DNA detection tools because of their superior sensitivity, fast response, and ease of operation [22,23]. Graphene has a high surface-to-volume ratio and ultra-high carrier mobility due to a single layer structure, making it a promising sensing material for DNA-FET sensors [24,25]. FETs could offer a limit of detection (LOD) of 100aM, which is based on target recycling and self-assembly amplification on GFET biosensors for multiplexed detection DNA [26]. Our previous work obtained LOD of 10aM, which molybdenum disulfide (MoS_2)/graphene nanostructure-based field-effect transistor was used for DNA detection. However, this work was a little tedious about MoS_2/graphene nanostructure fabrication [27]. Hence, Atmospheric pressure plasma jet (APPJ) is proposed for optimizing the performance of graphene to weaken the tedious fabrication process.

In this study, plasma treatment of the CVD graphene was firstly used on the solution-gated DNA-FET sensor to improve the affinity between target DNA and probe DNA, which could further promoted the sensitivity of DNA hybridization detection. A detection limit of 10 aM was obtained for the treated graphene-FET, which was an order of magnitude higher than that of untreated graphene-FET.

Atmospheric pressure plasma jet (APPJ) has been demonstrated that it is a low cost, low temperature, and rapid process for monolayer

* Corresponding author. School of Physics and Electronics, Shandong Normal University, Jinan, 250014, People's Republic of China.
** Corresponding author.
E-mail addresses: sdnupanjie@163.com (J. Pan), chengyang@sdnu.edu.cn (C. Yang).

https://doi.org/10.1016/j.talanta.2020.121766
Received 19 July 2020; Received in revised form 6 October 2020; Accepted 8 October 2020
Available online 18 October 2020
0039-9140/

graphene treatment [28]. Here, the room temperature APPJ, whose principles are expounded in our previous work [29,30], are designed to treat the CVD-graphene surface, as shown in Fig. 1a. Even at room temperature, the generated APPJ can generate a large number of electrons, ions, and radicals that can react to functionalize materials within a few seconds to minutes (Fig. S1) [31]. And such facile room temperature could avoid extreme application environment, reduce treatment time, and save costs. So that, DNA hybridization can be detected with the solution-gated GFET biosensors (Fig. 1b).

2. Experimental section

2.1. Material

The length of probe DNA, target DNA and mismatched DNA sequence were 30 base pairs, which were purchased from Sangon Biotech Inc.(Shanghai, China). 1-pyrenebutanoic acid succinimidyl ester (PBASE), phosphate buffer solution (PBS), the N,N-dimethylformamide (DMF), ethanolamine (EA), and polymethyl methacrylate (PMMA) were obtained from Aladdin. Other regents were ordered from Sinopharm Chemical Reagent Co., Ltd. Deionized (DI) water was obtained from a Millipore water purification system (Mili-Q Direct8).

2.2. Fabrication and treatment G-FET

Graphene was grown on Cu substrate via the chemical vapor deposition (CVD). It was obtained by using CVD with 50 sccm H_2 and 5 sccm CH_4 at 1050°*C*, and the deposition time was 30 min. PMMA coated on graphene/Cu substrate was used as a support layer to prevent graphene from tearing. Then, these graphene were soaked on ferric chloride ($FeCl_3$) solution ($FeCl_3$: deionized water = 27:100) to remove the Cu substrate. The soaking time was about 5 h. These PMMA/graphene films were cleaned three times in DI water and transferred onto the SiO_2/Si substrates, followed by the cleaning with acetone, ethanol, and DI water to remove the PMMA. Finally, indium tin oxide (ITO) was deposited and used as the source/drain electrodes with the area of sensing channel of 1 cm × 0.4 mm.

GFET was treated by the room temperature APPJ, based on pulse-modulated radio frequency with low atmospheric power consumption. This technique used a 2 KHz pulse generated by a pulse signal generator to modulate 13.56 MHz RF. The Ar gas flow was controlled to 3 L/min.

2.3. Device functionalization

The concentration of probe DNA was 1 uM and the concentration of target DNA was changed from 10 aM to 100 fM. PBASE dissolved in N,N-dimethylformamide for achieving the non-covalent functionalization was a linker reagent to bind graphene and probe DNA. 10 mM PBASE was added on the graphene channel surface for 6 h, then N,N-dimethylformamide and deionized water were used to washing the extra PBASE. 1 uM 5, -amino modification probe DNA was dropped on the channel to connect PBASE for 4 h, unbound DNAs were rinsed by PBS buffer solution. Finally, to defend possible nonspecific DNAs bound, 100 mM ethanolamine was used to eliminate the excessive unreacted groups of PBASE. Herein, the device had been modified. The different concentrations complementary DNA were dropped on the channel surface to hybridize with probe DNA and incubated for 4 h.

2.4. Characterizations

Atomic force microscopy (AFM) was used to demonstrate the changes of graphene. X-ray photoelectron spectroscopy (XPS) was used to characterize of the C_{1s} peak of graphene. Raman spectroscopy and UV–Visible spectroscopy were studied to analyze the optical properties. Keithley 4200-SCS semiconductor parameter analyzer was used to check the electrical properties.

3. Results and discussion

3.1. Performance of GFET

DNA hybridization detection can be measured by monitoring the voltage shift of the charge neutral point (ΔV_{CNP}), which several scans of voltage reached stabilization [32,33]. The humidity was kept at 50% which avoided to having an influence on the detecting process [34]. So that, the transfer characteristics curves of DNA hybridization for the GFET with (30 s, Fig. 2b) and without (Fig. 2a) plasma treatment were studied. From Fig. 2a and b, V_{CNP} of the GFET with and without plasma treatment were all shifted left as the concentration of complementary DNA increased from 10 aM to 100 fM. We believed that ΔV_{CNP} is mainly caused by the electron-rich bases in DNA molecules directly interact with the graphene, resulting in n-doping of graphene.

Obviously, ΔV_{CNP} of the treated GFET is much larger than that of the untreated GFET, which can be easily observed in Fig. 2a–c. Two reasons were considered here. First, the residues on the graphene surface without treatment, caused by the CVD graphene transfer, makes p-doping of graphene and weaken the shift of the V_{CNP}. However, plasma treatment of the graphene surface is useful to clean the residues and avoid the p-doping of the graphene [6], so that ΔV_{CNP} of the treated GFET is much larger. Another reason may be caused by the affinity reaction between target DNA and probe DNA on the graphene surface [35].

The affinity reaction between target DNA and probe DNA on the graphene surface was exhibited in Fig. 2d. DNA concentration (C_{DNA})/

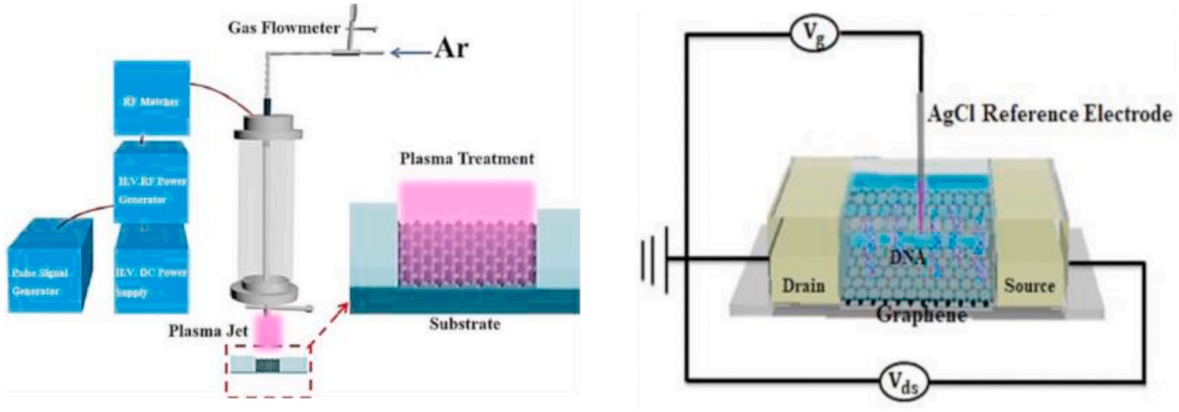

Fig. 1. (a) Schematic diagram of a room-temperature atmospheric pressure plasma jet based on pulsed modulated radio frequency (RF) technology. (b) Schematic of the solution-gated DNA-GFET sensor.

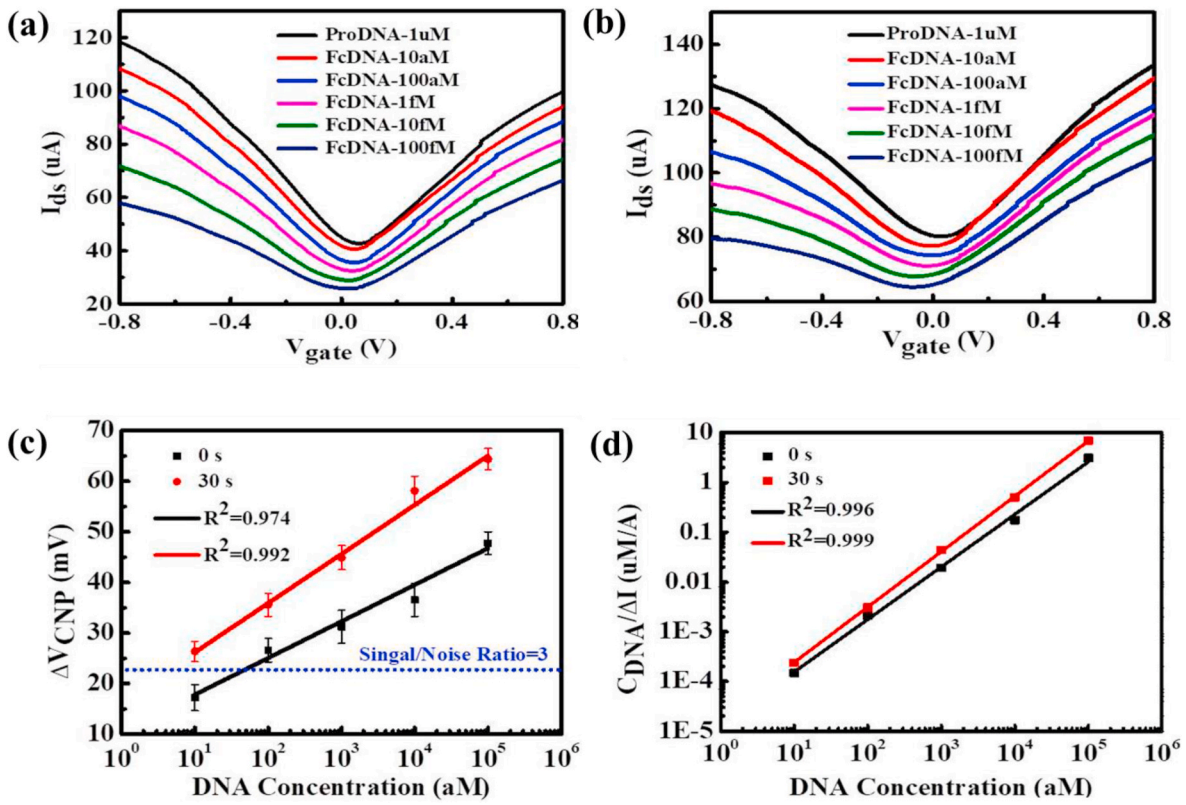

Fig. 2. (a) Transfer characteristics curves of the untreated GFET sensor. (b) Transfer characteristics curves of the treated GFET sensor with 30 s. (c) ΔV_{CNP} as a function of C_{DNA}. The dotted line indicates the third-level noise level of the blank control test. (d) $C_{DNA}/\Delta I$ as a function of C_{DNA}.

the amount of net drain current (ΔI) was plotted as a function of C_{DNA}. The adsorption of target DNA to probe DNA on the graphene channel follows the Langmuir adsorption isotherm [36]:

$$C_{DNA} / \Delta I_{sat} = C_{DNA}/\Delta I_{sat} + K_d/\Delta I_{sat} \quad (1)$$

K_d is the dissociation constant of reaction between probe DNA and target DNA, and ΔI_{sat} is the amount of saturated drain current. Through curve fitting, $K_d = 4.57 \times 10^{-9}$ M for untreated GFET was higher than $K_d = 3.84 \times 10^{-9}$ M for GFET treated with 30 s. The value of K_d is consistent with the results reported in the previous literature [37,38]. The reduction of K_d value demonstrated a better affinity between target DNA and probe DNA on the graphene surface.

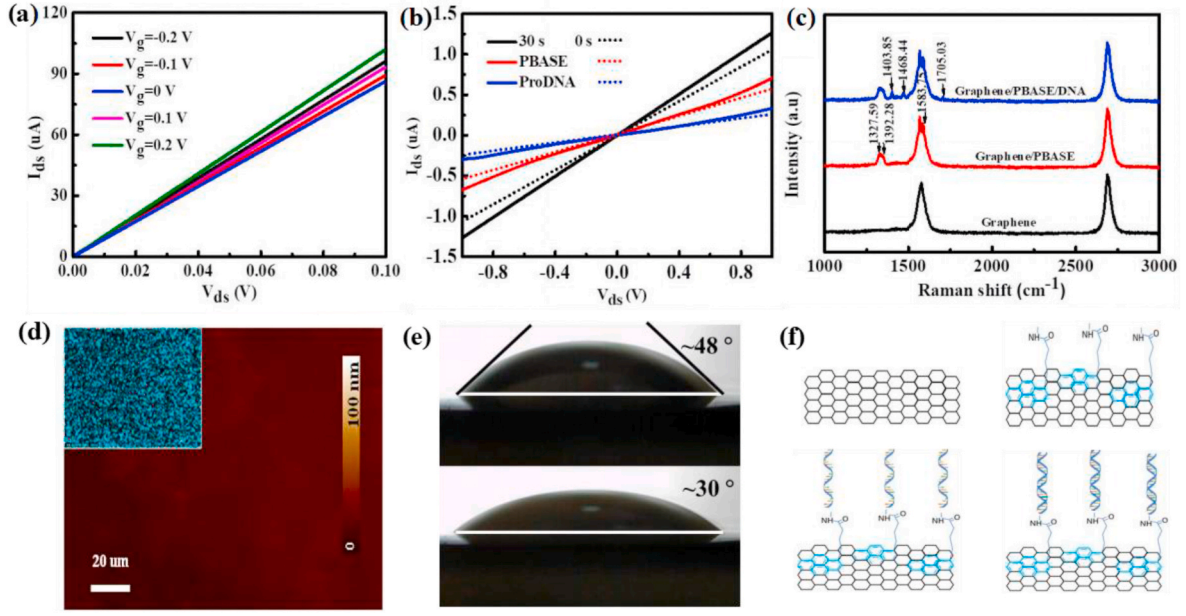

Fig. 3. (a) Output characteristics curves of the GFET biosensor treated with 30 s. (b) Output characteristics curves of GFET biosensors added with PBASE and probe DNA in sequence. (c) Raman spectroscopy of graphene during functionalization and hybridization. (d) AFM image of treated graphene with 30 s. Inset: EDS mapping image of C element. (e) Contact angle of graphene untreated and treated. (f) Flow chart of GFET biosensor surface functionalization.

ΔV_{CNP} can be used as the sensitivity detection signals to discuss the limit of detection (LOD), which was shown in Fig. 2c. LOD of 10 aM is given for the treated GFET, while LOD of 100 aM is obtained for the untreated GFET. An order of magnitude of the LOD was improved benefiting from the plasma treatment. As we all known, the detection signal of the lowest concentration of Fc DNA must be higher than the noise signal to be considered valid [39]. For the untreated GFET, the signal level (17.3 mV) of 10 aM DNA was lower than noise level (22.5 mV), which was less than 100 aM DNA (26.5 mV), so the data at 10 aM DNA was invalid.

3.2. Sensitivity of GFET and characterization of graphene

More details of the effects of the plasma treatment to the GFET sensors were analyzed by using I-V characteristics, Raman, AFM, EDS and contact angle detection. All of the plasma treatment is 30s here. The drain current fluctuated significantly with a slight change of gate voltage, as revealed in Fig. 3a. Variation of current indicated response of the biosensor was very sensitive to gate voltage and ohmic contacts between graphene and ITO electrodes [40]. Increased Current after treatment, suggested that treated GFET biosensor was more sensitive and more easily to detect electrical signals, as shown in Fig. 3b. AFM image (Fig. 3d) confirmed that residues on the graphene surface were removed. In addition, the inset EDS mapping of the C element was shown in Fig. 3d, which indicated that the graphene film is uniform.

3.3. Wettability of graphene and functionalization of GFET

PBASE solution was selected here as the linkage of probe DNA to graphene for hybridization detection, as depicted in Fig. 3c and f. PBASE was bound to graphene through π-π stacking. Probe aptamer will be immobilized by a conjugation reaction between probe DNA and the succinimide group of PBASE (Fig. S2). Finally, target DNA was hybridized with probe DNA. Graphene bound to DNA through PBASE was verified by Raman spectroscopy [41], as shown in Fig. 3c. The actual biomolecule detection carried out in solution, water molecules can easily affect the Fermi level of graphene as an external disturbance, which maybe leads noise signal and weak detection signals [27]. The blank control test (Fig.S3) revealed that transfer curves of GFET with or without DNA were almost overlapped, so the influence of noise was negligible.

The wettability of the graphene was changed by plasma treatment, which may be affective the adhesion between graphene interface and liquid interface. The contact angles of the graphene untreated and treated are shown in Fig. 3e. The contact angle in Young's equation is expressed as

$$\gamma_s = \gamma_{sl} + \gamma_l \cos\theta \tag{2}$$

γ_S, γ_l and γ_{sl} are solid surface free energy, liquid surface free energy and solid-liquid interface energy, respectively. θ is the angle between solid interface and liquid interface. The adhesion between solid interface and liquid interface can be described as

$$W_{sl} = \gamma_s + \gamma_l - \gamma_{sl} \tag{3}$$

Combine Equation (2) and Equation (3) to get Equation 4

$$W_{sl} = \gamma_s(1 + \cos\theta) \tag{4}$$

W_{sl} became larger with a contact angle from 48° to 30°, indicating that the adhesion was better between the treatment graphene and liquid [42]. Several reasons may be related to the wettability of the plasma treatment graphene: 1) Adhesive stress between graphene and the substrate is changed by the plasma treatment to change the wettability of graphene [43]; 2) Cleaning of the residues nanostructures on the graphene makes the graphene to hydrophilic [44]; 3) Some residues are oxidized by the APPJ plasma to form the hydrophilic functional groups [45].

3.4. APPJ treatment graphene

However, graphene could be damaged with many defects by the longer time treatment, plasma treatment time should be less than 30 s in our experiment. A series of tests with the different treatment time on graphene were studied. The optical transmittance of the graphene treated with 50 s is lower than that of 30 s (Fig. 4a). D band at ~1350 cm^{-1} of the Raman spectroscopy (Fig. 4b) of the graphene treated with 50 s is much higher than that of 30 s, which indicates the defect is generated by plasma treatment. And the position and intensity of the C_{1s} peak, which is related with the sp^2 bond of the carbon atoms, are changed and shown in Fig. 4c. Finally, The resistance of the graphene treated with 50s is also increased, which is shown in the I_{ds}-V_{ds} curve (Fig. 4d) and resistance changes (Fig. S4) of GFET.

Schematic diagram of the analytical model on the plasma treatment was revealed in the inset of Fig. 4e, which demonstrated energy transferred to graphene surface. With the assumption of the total energy E is

$$E = E_i + E_r \tag{5}$$

E_i is ion bombardment energy, and E_r is thermal energy generated by collision of electrons and ions. The total energy (U) accumulated over time (t) per unit area is

$$U = E_i n_i t_i + \int_0^t E r n_i dt - \int_{tl}^t q1 dt \tag{6}$$

n_i is ion density, t_i is the time when an atom suffered to bombard by ions and collide ions with electrons to lose energy with transition to adjacent atoms, t_1 is the time when the atom begins to release energy after gaining thermal energy saturation, and q_1 is the release rate per volume. Residues with O atoms can be removed with the Ar ion energy of 15.8 eV and the induced thermal energy Er. In the beginning, 15.8 eV of Ar ion energy is less than a minimum kinetic energy of 32 eV, which can be used to replace a carbon atom from graphene [46]. So that, carbon atoms can not replace from the graphene surface. However, E_r is increased with the increasing of the treatment time, which will destroy the graphene. In our experiment, the treatment time less than 30 s is important.

3.5. Specificity

The treated GFET biosensor with 30 s was used to detect three and thirty bases mismatched DNA, as revealed in Fig. 4f and S5. ΔV_{CNP} was increased as the increasing matched degree of complementary DNA for more complementary DNA was hybridized through specific adsorption with probe DNA. ΔV_{CNP} shift was very small when 30 Ms DNA hybridized with probe DNA, owing to non-specific adsorption between 30Ms DNA and probe DNA, which proved the GFET had highly specificity [47].

4. Conclusion

In summary, GFET biosensors based on plasma treatment were used for DNA hybridization detection which enhanced the affinity of target DNA and probe DNA. The electrical performance and the detection signal were improved due to removing residues on the surface of graphene. Herein, the plasma treatment time was explored and analyzed, which changed the hydrophilic properties of graphene and the adhesion of molecules to graphene. Moreover, the sensor had high sensitivity and LOD reached to 10 aM. Remarkably, the prepared FET had high specificity and could accurately recognize three bases mismatched DNA.

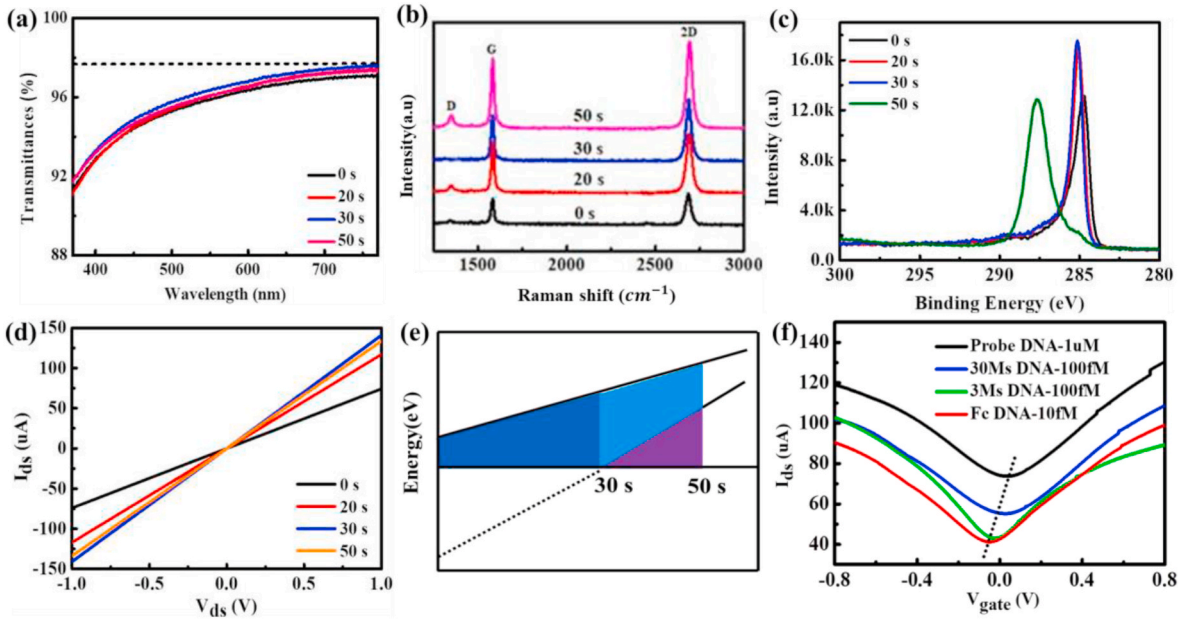

Fig. 4. Optical transmission spectra (a), Raman spectra (b) and XPS spectra (c) of graphene treated with different time, (d) Output characteristics curves of GFET biosensor treated with different time.(e) The schematic diagram of the analytical model to energy transfer to graphene surface with different time.(f)Transfer characteristics curves of treating GFET biosensor with complementary DNA, three bases mismatched DNA and thirty bases mismatched DNA.

Credit author statement

Yaping Xia: Conceptualization, Methodology, Software, Validation, Formal analysis, Investigation, Resources, Data curation, Writing - original draft, Visualization. Yang Sun and Huamin Li: Methodology, Investigation. Shuo Chen, Tiying Zhu and Guangcan Wang: Formal analysis, Software. Baoyuan Man and Jie Pan: Conceptualization, Writing - review & editing, Supervision. Cheng Yang: Conceptualization, Formal analysis, Resources, Data curation, Writing - review & editing, Supervision, Project administra-tion, Funding acquisition.

Declaration of competing interest

The authors declare that they have no known competing financial interests or personal relationships that could have appeared to influence the work reported in this paper.

Acknowledgments

This work was sponsored by the National Natural Science Foundation of China (11874244, 11974222) and Key Technology Research and Development Program of Shandong (Key Technology R&D Program of Shandong Province) (No. 2019GGX102048).

Appendix A. Supplementary data

Supplementary data to this article can be found online at https://doi.org/10.1016/j.talanta.2020.121766.

References

[1] M. Sivan, Y. Li, H. Veluri, Y. Zhao, B. Tang, X. Wang, E. Zamburg, J.F. Leong, J. X. Niu, U. Chand, A.V. Thean, All WSe_2 1T1R resistive RAM cell for future monolithic 3D embedded memory integration, Nat. Commun. 10 (1) (2019) 5201.
[2] I. Moon, S. Lee, M. Lee, C. Kim, D. Seol, Y. Kim, K.H. Kim, G.Y. Yeom, J. T. Teherani, J. Hone, W.J. Yoo, The device level modulation of carrier transport in a 2D WSe_2 field effect transistor via a plasma treatment, Nanoscale 11 (37) (2019) 17368–17375.
[3] J. Yu, A.A. Suleiman, Z. Zheng, X. Zhou, T. Zhai, Giant-enhanced SnS_2 photodetectors with broadband response through oxygen plasma treatment, Adv. Funct. Mater. 30 (24) (2020) 2001650.
[4] B.J. Lee, B.J. Lee, J. Lee, J.-W. Yang, K.-H. Kwon, Effects of plasma treatment on the electrical reliability of multilayer MoS_2 field-effect transistors, Thin Solid Films 637 (2017) 32–36.
[5] H. Li, A. Singh, F. Bayram, A.S. Childress, A.M. Rao, G. Koley, Impact of oxygen plasma treatment on carrier transport and molecular adsorption in graphene, Nanoscale 11 (23) (2019) 11145–11151.
[6] D. Ferrah, O. Renault, D. Marinov, J. Arias-Zapata, N. Chevalier, D. Mariolle, D. Rouchon, H. Okuno, V. Bouchiat, G. Cunge, CF4/H2 plasma cleaning of graphene regenerates electronic properties of the pristine material, ACS Appl. Nano Mater. 2 (3) (2019) 1356–1366.
[7] B.-J. Lee, G.-H. Jeong, Efficient surface functionalization of vertically-aligned carbon nanotube arrays using an atmospheric pressure plasma jet system, Fullerenes, Nanotub. Carbon Nanostruct. 26 (2) (2018) 116–122.
[8] Q. Yuan, S. Wu, C. Ye, X. Liu, J. Gao, N. Cui, P. Guo, G. Lai, Q. Wei, M. Yang, W. Su, H. Li, N. Jiang, L. Fu, D. Dai, C.-T. Lin, K.W.A. Chee, Sensitivity enhancement of potassium ion (K+) detection based on graphene field-effect transistors with surface plasma pretreatment, Sensor. Actuator. B Chem. 285 (2019) 333–340.
[9] U.V. Patil, A.S. Pawbake, L.G.B. Machuno, R.V. Gelamo, S.R. Jadkar, C.S. Rout, D. J. Late, Effect of plasma treatment on multilayer graphene: X-ray photoelectron spectroscopy, surface morphology investigations and work function measurements, RSC Adv. 6 (54) (2016) 48843–48850.
[10] D. Ghosh, L.P. Datta, T. Govindaraju, Molecular architectonics of DNA for functional nanoarchitectures, Beilstein J. Nanotechnol. 11 (2020) 124–140.
[11] Y. Yu, Q. Zhu, F. Xiang, Y. Hu, L. Zhang, X. Xu, N. Liu, S. Huang, Applying AuNPs/SWCNT to fabricate electrical nanogap device for DNA hybridization detection, Carbon 157 (2020) 40–46.
[12] P. Carneiro, S. Morais, M. do Carmo Pereira, Biosensors on the road to early diagnostic and surveillance of Alzheimer's disease, Talanta 211 (2020) 120700.
[13] Z. Luo, Y. Xu, Z. Huang, J. Chen, X. Wang, D. Li, Y. Li, Y. Duan, A rapid, adaptative DNA biosensor based on molecular beacon-concatenated dual signal amplification strategies for ultrasensitive detection of p53 gene and cancer cells, Talanta 210 (2020) 120638.
[14] D.V. Verschueren, S. Pud, X. Shi, L. De Angelis, L. Kuipers, C. Dekker, Label-free optical detection of DNA translocations through plasmonic nanopores, ACS Nano 13 (1) (2019) 61–70.
[15] R. Tian, W. Ning, M. Chen, C. Zhang, Q. Li, J. Bai, High performance electrochemical biosensor based on 3D nitrogen-doped reduced graphene oxide electrode and tetrahedral DNA nanostructure, Talanta 194 (2019) 273–281.
[16] R. Salimian, S. Shahrokhian, S. Panahi, Enhanced electrochemical activity of a hollow carbon sphere/polyaniline-based electrochemical biosensor for HBV DNA marker detection, ACS Biomater. Sci. Eng. 5 (5) (2019) 2587–2594.
[17] K. Wen, X. Yang, C. Zhang, H. Wei, G. Zou, Y. Zhu, Exonuclease III-assisted positive feedback signal amplification strategy for ultrasensitive electrochemical detection of nucleic acids, Sensor. Actuator. B Chem. 304 (2020) 127410.
[18] F. Feng, W. Chen, D. Chen, W. Lin, S.-C. Chen, In-situ ultrasensitive label-free DNA hybridization detection using optical fiber specklegram, Sensor. Actuator. B Chem. 272 (2018) 160–165.
[19] T.T.V. Nguyen, X. Xie, J. Xu, Y. Wu, M. Hong, X. Liu, Plasmonic bimetallic nanodisk arrays for DNA conformation sensing, Nanoscale 11 (41) (2019) 19291–19296.

[20] D. Kawasaki, K. Maeno, H. Yamada, K. Sueyoshi, H. Hisamoto, T. Endo, TiN-contained polymer-metal core-shell structured nanocone array: engineering of sensor performance by controlling plasmonic properties, Sensor. Actuator. B Chem. 299 (2019) 126932.
[21] S. Xu, S. Jiang, C. Zhang, W. Yue, Y. Zou, G. Wang, H. Liu, X. Zhang, M. Li, Z. Zhu, J. Wang, Ultrasensitive label-free detection of DNA hybridization by sapphire-based graphene field-effect transistor biosensor, Appl. Surf. Sci. 427 (2018) 1114–1119.
[22] S. Lai, M. Barbaro, A. Bonfiglio, The role of polarization-induced reorientation of DNA strands on organic field-effect transistor-based biosensors sensitivity at high ionic strength, Appl. Phys. Lett. 107 (10) (2015).
[23] Z. Wang, Y. Jia, Graphene solution-gated field effect transistor DNA sensor fabricated by liquid exfoliation and double glutaraldehyde cross-linking, Carbon 130 (2018) 758–767.
[24] S. Li, K. Huang, Q. Fan, S. Yang, T. Shen, T. Mei, J. Wang, X. Wang, G. Chang, J. Li, Highly sensitive solution-gated graphene transistors for label-free DNA detection, Biosens. Bioelectron. 136 (2019) 91–96.
[25] D. Han, R. Chand, Y.S. Kim, Microscale loop-mediated isothermal amplification of viral DNA with real-time monitoring on solution-gated graphene FET microchip, Biosens. Bioelectron. 93 (2017) 220–225.
[26] Z. Gao, H. Xia, J. Zauberman, M. Tomaiuolo, J. Ping, Q. Zhang, P. Ducos, H. Ye, S. Wang, X. Yang, F. Lubna, Z. Luo, L. Ren, A.T.C. Johnson, Detection of sub-fM DNA with target recycling and self-assembly amplification on graphene field-effect biosensors, Nano Lett. 18 (6) (2018) 3509–3515.
[27] S. Chen, Y. Sun, Y. Xia, K. Lv, B. Man, C. Yang, Donor effect dominated molybdenum disulfide/graphene nanostructure-based field-effect transistor for ultrasensitive DNA detection, Biosens. Bioelectron. 156 (2020) 112128.
[28] C.-H. Huang, T.-H. Lu, Rapid oxidation of CVD-grown graphene using mild atmospheric pressure O2 plasma jet, Surf. Coating. Technol. 350 (2018) 1085–1090.
[29] Y. Zhao, C. Wang, L. Li, L. Wang, J. Pan, Reaction pathways of producing and losing particles in atmospheric pressure methane nanosecond pulsed needle-plane discharge plasma, Phys. Plasmas 25 (3) (2018).
[30] J. Du, Z. Liu, C. Bai, L. Li, Y. Zhao, L. Wang, J. Pan, Concentration distributions and reaction pathways of species in the mass transfer process from atmospheric pressure plasma jet to water, Eur. Phys. J. D 72 (10) (2018).
[31] B.M. Foley, S.C. Hernandez, J.C. Duda, J.T. Robinson, S.G. Walton, P.E. Hopkins, Modifying surface energy of graphene via plasma-based chemical functionalization to tune thermal and electrical transport at metal interfaces, Nano Lett. 15 (8) (2015) 4876–4882.
[32] C.-T. Lin, P.T.K. Loan, T.-Y. Chen, K.-K. Liu, C.-H. Chen, K.-H. Wei, L.-J. Li, Label-free electrical detection of DNA hybridization on graphene using Hall effect measurements: revisiting the sensing mechanism, Adv. Funct. Mater. 23 (18) (2013) 2301–2307.
[33] M.T. Hwang, M. Heiranian, Y. Kim, S. You, J. Leem, A. Taqieddin, V. Faramarzi, Y. Jing, I. Park, A.M. van der Zande, S. Nam, N.R. Aluru, R. Bashir, Ultrasensitive detection of nucleic acids using deformed graphene channel field effect biosensors, Nat. Commun. 11 (1) (2020) 1543.
[34] G. Wu, X. Tang, M. Meyyappan, K.W.C. Lai, Doping effects of surface functionalization on graphene with aromatic molecule and organic solvents, Appl. Surf. Sci. 425 (2017) 713–721.
[35] M.A. von Keyserlingk, A. Barrientos, K. Ito, E. Galo, D.M. Weary, Benchmarking cow comfort on North American freestall dairies: lameness, leg injuries, lying time, facility design, and management for high-producing Holstein dairy cows, J. Dairy Sci. 95 (12) (2012) 7399–7408.
[36] Y. Sun, Z. Peng, H. Li, Z. Wang, Y. Mu, G. Zhang, S. Chen, S. Liu, G. Wang, C. Liu, L. Sun, B. Man, C. Yang, Suspended CNT-Based FET sensor for ultrasensitive and label-free detection of DNA hybridization, Biosens. Bioelectron. 137 (2019) 255–262.
[37] C. Zheng, L. Huang, H. Zhang, Z. Sun, Z. Zhang, G.J. Zhang, Fabrication of ultrasensitive field-effect transistor DNA biosensors by a directional transfer technique based on CVD-grown graphene, ACS Appl. Mater. Interfaces 7 (31) (2015) 16953–16959.
[38] Q. Su, S. Vogt, G. Noll, Langmuir analysis of the binding affinity and kinetics for surface tethered duplex DNA and a ligand-apoprotein complex, Langmuir 34 (49) (2018) 14738–14748.
[39] J. Mei, Y.T. Li, H. Zhang, M.M. Xiao, Y. Ning, Z.Y. Zhang, G.J. Zhang, Molybdenum disulfide field-effect transistor biosensor for ultrasensitive detection of DNA by employing morpholino as probe, Biosens. Bioelectron. 110 (2018) 71–77.
[40] F. Mirzaii Babolghani, E. Mohammadi-Manesh, Simulation and experimental study of FET biosensor to detect polycyclic aromatic hydrocarbons, Appl. Surf. Sci. 488 (2019) 662–670.
[41] S. Xu, J. Zhan, B. Man, S. Jiang, W. Yue, S. Gao, C. Guo, H. Liu, Z. Li, J. Wang, Y. Zhou, Real-time reliable determination of binding kinetics of DNA hybridization using a multi-channel graphene biosensor, Nat. Commun. 8 (2017) 14902.
[42] S. Wang, Y. Zhang, N. Abidi, L. Cabrales, Wettability and surface free energy of graphene films, Langmuir 25 (18) (2009) 11078–11081.
[43] N.N. Nguyen, S.B. Jo, S.K. Lee, D.H. Sin, B. Kang, H.H. Kim, H. Lee, K. Cho, Atomically thin epitaxial template for organic crystal growth using graphene with controlled surface wettability, Nano Lett. 15 (4) (2015) 2474–2484.
[44] D.Y. Wang, I.S. Huang, P.H. Ho, S.S. Li, Y.C. Yeh, D.W. Wang, W.L. Chen, Y.Y. Lee, Y.M. Chang, C.C. Chen, C.T. Liang, C.W. Chen, Clean-lifting transfer of large-area residual-free graphene films, Adv. Mater. 25 (32) (2013) 4521–4526.
[45] S.-H. Chang, J.-S. Liou, J.-L. Liu, Y.-F. Chiu, C.-H. Xu, B.-Y. Chen, J.-Z. Chen, Feasibility study of surface-modified carbon cloth electrodes using atmospheric pressure plasma jets for microbial fuel cells, J. Power Sources 336 (2016) 99–106.
[46] Y.-D. Lim, D.-Y. Lee, T.-Z. Shen, C.-H. Ra, J.-Y. Choi, W.-J. Yoo, Si-compatible cleaning process for graphene using low-density inductively coupled plasma, ACS Nano 6 (2012) 4410–4417.
[47] J. Liu, X. Chen, Q. Wang, M. Xiao, D. Zhong, W. Sun, G. Zhang, Z. Zhang, Ultrasensitive monolayer MoS_2 field-effect transistor based DNA sensors for screening of down syndrome, Nano Lett. 19 (3) (2019) 1437–1444.